Highly Selective Ammonia Synthesis from Nitrate with Photocatalytically Generated Hydrogen on CuPd/TiO2

5 AUTHORS, INCLUDING:

Ryu Abe

Kyoto University

113 PUBLICATIONS **5,592** CITATIONS

Highly Selective Ammonia Synthesis from Nitrate with Photocatalytically Generated Hydrogen on CuPd/TiO$_2$

Miho Yamauchi,*,[†,‡,§,∥] Ryu Abe,[†,‡,§] Tatsuya Tsukuda,[†] Kenichi Kato,[§,∥,⊥] and Masaki Takata[∥,⊥]

[†]CRC, Hokkaido University, Nishi 10, Kita 21, Kita-ku, Sapporo 001-0021, Japan
[‡]JST-PRESTO, Sanbancho 5, Chiyoda-ku, Tokyo 102-0075, Japan
[§]JST-CREST, Sanbancho 5, Chiyoda-ku, Tokyo 102-0075, Japan
[∥]RIKEN SPring-8 Center, 1-1-1 Kouto, Sayo-gun, Hyogo 679-5148, Japan
[⊥]Japan Synchrotron Radiation Research Institute, 1-1-1 Kouto, Sayo-gun, Hyogo 679-5148, Japan

S *Supporting Information*

ABSTRACT: Body-centered-cubic type CuPd nanoalloys were synthesized by a chemical reduction method. Photocatalytic hydrogen evolution and nitrate reduction were simultaneously examined over CuPd nanoalloys deposited on TiO$_2$ (CuPd/TiO$_2$). The efficiency of hydrogen evolution over CuPd/TiO$_2$ was better than that over Pd/TiO$_2$. As for nitrate reduction, ammonia was selectively (78%) produced with hydrogen generated photocatalytically over CuPd/TiO$_2$. The continuous generation of nascent hydrogen atoms on the surface of the CuPd nanoalloy, where Cu and Pd are homogeneously mixed, led to the high selectivity for ammonia.

Ammonia (NH$_3$) is a main component in chemical fertilizers and recently has been noted as an energy carrier for alkaline fuel cells.[1] In the present world, which is confronted with both a food and energy crises, greater demand for NH$_3$ is therefore forecasted.[2] In industrial NH$_3$ production, however, huge amounts of fossil fuels, especially natural gas, are consumed to produce H$_2$, while equally large amounts of CO$_2$ are released. Fossil fuel-free H$_2$ gas produced based on renewable energy sources, such as photocatalytically generated H$_2$ from water utilizing solar light,[3] has therefore received much attention as a clean energy carrier, as well as a raw material for various chemicals production processes, including that for NH$_3$. At the same time, overmanuring with synthetic fertilizers causes an increase in the concentration of nitrate ion (NO$_3^-$) and its derivatives in groundwater.[4] Here, we performed the reduction of NO$_3^-$ into NH$_3$ with photocatalytically generated hydrogen as another environmentally benign process that could produce NH$_3$ without releasing CO$_2$ and consuming excess energy.

The catalytic reduction of NO$_3^-$ into nitrogen (N$_2$) with H$_2$ has been investigated as an ideal detoxifying process.[5] Copper—palladium (CuPd) bimetallic alloy nanoparticles loaded on a support are known to be active for NO$_3^-$ reduction into N$_2$ in the presence of hydrogen dissolved in solution. It has been proposed that the NO$_3^-$ ions are first reduced to nitrite ions (NO$_2^-$) on the bimetallic CuPd surface.[5] Then, NO$_2^-$ is reduced to N$_2$ or NH$_3$. Previous reports suggested that the

distribution of Pd and Cu in the bimetallic particles dictate the selectivity in the latter step. On the particulate alloys where Pd atoms form relatively large domains, NO$_2^-$ is preferentially reduced into N$_2$.[6] On the other hand, NH$_3$ generation appears to preferentially occur on the well mixed alloy surfaces.[6] In order to prepare homogeneously mixed nanoalloys, we synthesized CuPd alloy nanoparticles first, which we then deposited on a TiO$_2$ support. CuPd nanoalloys were produced by a chemical reduction method using poly[n-vinyl-2-pyrrolidone] (PVP) as a protective reagent to control the alloy size.[7] Characterization of the sample was performed by inductively coupled plasma atomic emission spectrometry (ICP-AES), TEM, and powder XRD. The molar composition of the alloy was determined by ICP-AES to be Cu/Pd = 52:48. Based on the TEM image shown in Figure S1a, the CuPd nanoalloys were found to have a moniliform structure. The largest width of each bulge in the sample was taken for the static values of their sizes. Average sizes of the CuPd nanoalloys and Pd nanoparticles were determined to be 5.6 ± 1.7 and 4.3 ± 0.7 nm, respectively. TEM images of the CuPd nanoalloy taken using high magnification are shown in Figure S1b and c. The distorted lattice fringe as shown in Figure S1b indicates that the crystallinity of the CuPd nanoalloy is quite low. The TEM image in Figure S1c was taken along the [001] zone axis of the center part of the field of vision. The d-spacing of {001} was estimated to be 0.305 nm.

The XRD pattern of a prepared sample is displayed in Figure 1a.[8] Although both metals have an fcc structure in the bulk state, the XRD pattern of the nanoalloy could be reproduced assuming a bcc-type structure. This implies that the nanoalloy is constructed of a homogeneous mixture of Cu and Pd atoms, and not by a mixture of Cu and Pd clusters. The lattice constant was determined to be 3.096(10) Å by Rietveld profile analysis assuming a B2-type ordered alloy structure. This lattice constant agrees with the {001} d-spacing observed in the TEM image, implying that the CuPd nanoalloy has bcc-type symmetry. This value is larger by 0.1 Å than the constant for bulk B2-type CuPd (2.99 Å). In previous reports,[9] we proposed that the atomic arrangement in as-prepared Pd nanoparticles is disordered and characterized by a large lattice constant due to the extra volume generated in the disordered lattice. We think a similar phenomenon
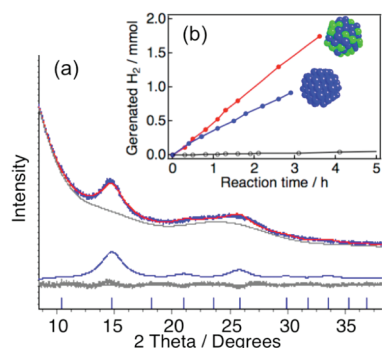
Figure 1. (a)Powder XRD pattern and Rietveld profile of the CuPd nanoalloy. The observed pattern (blue) was reproduced by the curve calculated assuming a B2-type structure (*lattice const.* = 3.096(10) Å, *diameter* = 2.0(6) nm, Rw = 1.57%, GOF = 1.56) (red). (b) Time courses of hydrogen evolution over CuPd/TiO$_2$ (red), Pd/TiO$_2$ (blue), and TiO$_2$ (○).

may occur in the CuPd nanoalloy. It should be mentioned that even though the most stable structure of bulk CuPd in an equal Cu—Pd alloy composition is an ordered B2-type structure,[10] the small crystalline size of the CuPd nanoalloy avoids an exact attribution to ordered-B2 or disordered-bcc types.

In this study, TiO$_2$, which is a conventional photocatalyst, was selected as a support semiconductor. Photocatalysts were prepared by simple mixing of TiO$_2$ powder (AEROXIDE, TiO$_2$ P25) and an aqueous solution of the CuPd nanoalloy. As a reference sample, we also prepared a catalyst with PVP-coated Pd nanoparticles (Pd/TiO$_2$) with the same molar metal content as that in CuPd/TiO$_2$. The commonly used CuPd bimetallic catalyst (*n*-CuPd/TiO$_2$) was prepared using the impregnation method.[11] Photocatalytic hydrogen generation and NO$_3^-$ reduction under UV irradiation (λ > 300 nm) were carried out in the presence of methanol as a sacrificial electron donor after substitution of argon for air in the reaction system. To avoid dispersion of NH$_3$ into the gas phase, the temperature of the reaction vessel was maintained at 290 K using a water bath equipped with a recirculation chiller. It was first determined that NO$_3^-$ was not reduced over CuPd/TiO$_2$ in the absence of H$_2$(g) and UV irradiation. As separate control reactions, we examined NO$_3^-$ reduction without UV irradiation, *i.e*, in the dark, but with ca. 350 Torr of added H$_2$(g), which corresponds to twice the amount of hydrogen generated under UV irradiation for 3 h. The concentrations of NO$_3^-$, NO$_2^-$, and NH$_3$ in the solution and an amount of generated N$_2$ in the gas phase were determined by ion chromatography and gas chromatography, respectively.

Time courses of hydrogen evolution over CuPd/TiO$_2$, Pd/TiO$_2$, and TiO$_2$ are shown in Figure 1b. The amount of H$_2$ evolved over CuPd/TiO$_2$ was found to be greater than that over TiO$_2$ and Pd/TiO$_2$. These results indicate that, similar to Pd, CuPd nanoalloys act as an effective cocatalyst for hydrogen production from water containing 10 vol% methanol.

It is notable that CuPd/TiO$_2$ including Cu by the amount of a half atomic percentage of the nanoalloy showed an excellent activity, higher than that of Pd/TiO$_2$. Percentages of residual NO$_3^-$, generated NO$_2^-$, and NH$_3$ to the initial concentration of NO$_3^-$ in the reaction solutions are shown in Figure 2.[12] During the reaction over Pd/TiO$_2$ in the dark, almost none of products are generated (a). Under UV irradiation, a small amount of NO$_3^-$ ions was converted, 15% of them to NH$_3$ (b). Compared to the results for Pd/TiO$_2$, larger amounts of NO$_3^-$ were
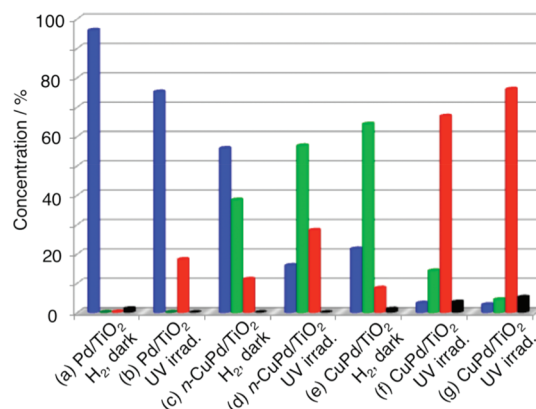

Figure 2. Concentrations of NO$_3^-$ (blue), NO$_2^-$ (green), NH$_3$ (red), and N$_2$ (black) relative to the initial NO$_3^-$ concentration after reaction in a 470 μM NO$_3^-$ aqueous solution including 10 vol% methanol. The catalytic reactions were conducted with the following: (a) Pd/TiO$_2$ (0.46 wt %) with H$_2$ in the dark and (b) under UV irradiation, (c) *n*-CuPd/TiO$_2$ (0.37 wt %) with H$_2$ in the dark and (d) under UV irradiation, and (e) CuPd/TiO$_2$ (0.37 wt %) with H$_2$ in the dark and (f and g) under UV irradiation. Reaction time for (a—f) was 3 h and that for (g) is 5 h.

converted to NO$_2^-$ and NH$_3$ over *n*-Cu—Pd/TiO$_2$ in the dark (c). Under UV irradiation, 28% of NO$_3^-$ was converted to NH$_3$ (d). In the reaction over CuPd/TiO$_2$ in the dark, NO$_2^-$ ions were found to be the main product with a concentration of 64% and a small amount of NH$_3$ was detected (e). On the other hand, large amounts of NH$_3$ were produced under UV irradiation (f). After 5 h of irradiation, all of NO$_3^-$ ions were converted and NH$_3$ was identified as a product with a concentration of 76% (g). This value is higher than 28% in the photocatalytic NO$_3^-$ reduction over *n*-Cu—Pd/TiO$_2$ (d).[11a,13] Conversion of NO$_3^-$ ions over CuPd/TiO$_2$ always resulted in small percentages of residual NO$_3^-$ (e, f, g), implying that, similarly to previously reported results,[5,6] CuPd bimetallic alloys showed high catalytic activity for NO$_3^-$ reduction both in the dark and under UV irradiation. Although the amount of NH$_3$ in the gas phase could not be determined in our experiments, the yield for NH$_3$ over CuPd/TiO$_2$ under UV irradiation for 5 h was found to be 76% (g), which corresponds to 78% of selectivity. These results indicate that utilization of photocatalytically generated hydrogen leads to high selectivity for NH$_3$ in the reduction of NO$_3^-$. The quantum yields for H$_2$ and NH$_3$ production over CuPd/TiO$_2$ were determined to be 10.2 and 0.22% in the reaction under irradiation of 365 nm monochromatic light.

Next, we examined reactions over CuPd/TiO$_2$ using an initial concentration of NO$_3^-$ ions that was 5 times higher than previously employed. In Table S1, reduced concentrations of NO$_3^-$ and concentrations of produced NO$_2^-$ and NH$_3$ after reaction for 3 h in the dark and under UV irradiation are tabulated. Ratios of these concentrations detected under UV irradiation and in the dark are also shown. The reduction of NO$_3^-$ concentration appeared to be almost linear compared to the initial concentration of NO$_3^-$ and was not affected by UV irradiation. When the initial concentration of NO$_3^-$ was disregarded, the amount of generated NH$_3$ was found to be 8—9 times more for reactions under photoirradiation than that obtained in the dark. These results suggest that NO$_3^-$ reduction is not influenced by UV irradiation but NO$_2^-$ reduction to NH$_3$ is much accelerated.

To rationalize the high selectivity to NH_3 observed in the reaction over $CuPd/TiO_2$ under UV irradiation, we propose two explanations. First is the homogeneous mixing of Cu and Pd on the surface of the alloy. Hydrogenation of NO_2^- is considered to be a critical step controlling selectivity toward N_2 and NH_3.[14] As discussed above, we found that Cu and Pd atoms are homogeneously distributed in the CuPd nanoalloy. The percentage of single Pd sites where a Pd atom is directly surrounded by copper atoms is possibly large, resulting in highly selective NH_3 production.[15] Thus, it can be said that detailed structural design of the nanoalloy is required for the creation of highly efficient catalysts.[16] Second, is the high hydrogenation ability of photocatalytically generated hydrogen. The selectivity of NO_2^- hydrogenation over CuPd nanoalloys can be connected to the ratio of reductant species to the surface coverage of N species, H/N.[5d,6] Given that the amount of hydrogen evolved on $CuPd/TiO_2$ is larger than that on Pd/TiO_2, it is likely that hydrogen atoms are generated not only in the proximity of Pd sites but also around Cu sites. It is, hence, supposed that nitrogen oxides absorbed on the surface are continuously surrounded by nascent hydrogen atoms unremittingly. In such a case, a high H/N ratio is attained, resulting in the high selectivity to NH_3.

In the present study, it was found that photocatalytically generated hydrogen exhibits high selectivity for conversion of NO_3^- to NH_3. This ability can be ascribed to a flux of nascent hydrogen surrounding the substrates. Highly selective NH_3 production via NO_3^- reduction using hydrogen evolved by solar energy represents a promising approach for fossil-free NH_3 production from waste treatment.

■ ASSOCIATED CONTENT

Ⓢ Supporting Information. Experimental details, TEM image, XRD patterns, IR spectra, and catalytic activities of $CuPd/TiO_2$ for NO_3^- reduction. This material is available free of charge via the Internet at http://pubs.acs.org.

■ AUTHOR INFORMATION

Corresponding Author
yamauchi@cat.hokudai.ac.jp

■ ACKNOWLEDGMENT

■ REFERENCES

(1) Erisman, J. W.; Sutton, M. A.; Galloway, J.; Klimont, Z.; Winiwarter, W. *Nat. Geosci.* **2008**, *1*, 636–639.

(2) Jennings, J. R. *Catalytic Ammonia Synthesis, Fundamentals and practice*; Plenum Press: New York, 1991.

(3) Abe, R.; Higashi, M.; Domen, K. *J. Am. Chem. Soc.* **2010**, *132*, 11828–11829.

(4) (a) Murphy, A. P. *Nature* **1991**, *350*, 223–225. (b) Fanning, J. C. *Coord. Chem. Rev.* **2000**, *199*, 159–179.

(5) (a) Vorlop, K.-D.; Tacke, T. *Chem. Ing. Tech.* **1989**, *61*, 836–837. (b) Hörold, S.; Vorlop, K.-D.; Tacke, T.; Shell, M. *Catal. Today* **1993**, *17*, 21–30. (c) Prüsse, U.; Hähnlein, M.; Daum, J.; Vorlop, K.-D. *Catal. Today* **2000**, *55*, 79–90. (d) Prüsse, U.; Vorlop, K.-D. *J. Mol. Catal. A: Chem.* **2001**, *173*, 313–328. (e) Pinter, A.; Batista, J.; Levec, J.; Kajiuchi, T. *Appl. Catal., B* **1996**, *11*, 81–98. (f) Sakamoto, Y.; Kanno, M.; Okuhara, T.; Kamiya, Y. *Cata. Lett.* **2008**, *125*, 392–395.

(6) Yoshinaga, Y.; Akita, T.; Mikami, I.; Okuhara, T. *J. Catal.* **2002**, *207*, 37–45.

(7) Teranishi, T.; Miyake, M. *Chem. Mater.* **1998**, *10*, 594–600.

(8) Kato, K.; Hirose, R.; Takemoto, M.; Ha, S.; Kim, J.; Higuchi, M.; Matsuda, R.; Kitagawa, S.; Takata, M. AIP Conference Proceedings 2010, 1234, 867–870.

(9) (a) Yamauchi, M.; Kobayashi, H.; Kitagawa, H. *ChemPhysChem* **2009**, *10* (15), 2566–2576. (b) Yamauchi, M.; Ikeda, R.; Kitagawa, H.; Takata, M. *J. Phys. Chem. C* **2008**, *112* (9), 3294–3299. (c) Yamauchi, M.; Kitagawa, H. *Synth. Met.* **2005**, *153*, 353–356.

(10) Friedrich, M.; Armbrüster, M. *Chem. Mater.* **2009**, *21*, 5886–5891.

(11) (a) Sá, J.; Berger, T.; Föttinger, K.; Riss, A.; Anderson, J. A.; Vinek, H. *J. Catal.* **2005**, *234*, 282–291. (b) Gao, W.; Guan, N.; Chen, J.; Guan, X.; Jin, R.; Zeng, H.; Liu, Z.; Zhang, F. *Appl. Catal., B* **2003**, *46*, 341–351.

(12) N balances were determined within a ±7% error range for reactions (a), (b), (c), (d), and (e). However, total concentrations of N-containing species in reaction solutions (f) and (g) are still too low by 12%, i.e., 88%. Considering that the catalytic reactions under UV irradiation were performed at low pressures, e.g., less than 100 Torr, this disagreement observed in (f) and (g) where a large amount of NH_3 was produced can possibly be attributed to gaseous NH_3 dispersed in the closed glass gas circulation system, for which we could not determine the concentration.

(13) (a) Wehbe, N.; Jaafar, M.; Guillard, C.; Herrmann, J.-M.; Miachon, S.; Puzenat, E.; Guilhaume, N. *Appl. Catal., A* **2009**, *368*, 1–8. (b) Ranjit, K. T.; Viswanathan, B. *J. Photochem. Photobiol., A* **1997**, *108*, 73–78. (c) Li, Y.; Wasgestian, F. *J. Photochem. Photobiol., A* **1998**, *112* (2−3), 255–259.

(14) (a) Ilinitch, O. M.; Cuperus, F. P.; Nosova, L. V.; Gribov, E. N. *Catal. Today* **2000**, *56*, 137–145. (b) Mikami, I.; Sakamoto, Y.; Yoshinaga, Y.; Okuhara, T. *Appl. Catal., B* **2003**, *44*, 79–86.

(15) (a) Zang, F.; Miao, S.; Yang, Y.; Zang, X.; Chen, J.; Guan, N. *J. Phys. Chem. C* **2008**, *112*, 7665–7671. (b) Deganello, F.; Liotta, L. F.; Macaluso, A.; Venezia, A. M.; Deganello, G. *Appl. Catal., B* **2000**, *24*, 265–273.

(16) Alayoglu, S.; Nilekar, U. A.; Mavrikakis, M.; Eichhorn, B. *Nat. Mater.* **2008**, *7*, 333–338.

C

dx.doi.org/10.1021/ja106285p |*J. Am. Chem. Soc.* XXXX, XXX, 000–000